

HUNTING DOWN THE QUARK-GLUON PLASMA IN RELATIVISTIC HEAVY-ION COLLISIONS

ULRICH HEINZ^{a,b}

^a *Theory Division, CERN, CH-1211 Geneva 23, Switzerland
E-mail: Ulrich.Heinz@cern.ch*

^b *Institut für Theoretische Physik, Universität Regensburg,
D-93040 Regensburg, Germany*

The present status of the heavy-ion program to search for quark-gluon plasma is reviewed. The goal of this program is to recreate the Big Bang in the laboratory, by generating small chunks of exploding quark-gluon plasma (“The Little Bang”). I argue that the analogues of the three pillars of Big Bang Theory (Hubble flow, microwave background radiation, and primordial nucleosynthesis) have now been firmly established in heavy-ion collisions at SPS energies: there is convincing evidence for strong radial flow, thermal hadron emission, and primordial hadrosynthesis from a color-deconfined initial stage. Direct observation of the quark-gluon plasma phase via its electromagnetic radiation will be possible in planned collider experiments at higher energies.

1 Introduction: What Are We Looking For?

The highest particle and energy densities existed for a fleeting moment in the early history of our universe, shortly after the “Big Bang”. In heavy-ion collisions at ultrarelativistic energies one hopes to be able to recreate such high-density matter and to study its properties. At presently available beam energies the goal is to pass the energy density threshold for color-deconfinement¹, $\epsilon_{\text{cr}} \lesssim 1 \text{ GeV/fm}^3$. If such energy densities can be reached and the energy sufficiently thermalized, strongly interacting matter will manifest itself as a **quark-gluon plasma**: the hadronic constituents (quarks and gluons) become deconfined, and hadrons lose their identity.

1.1 The Big Bang model as an example

How do we know that high energy densities existed in the Early Universe? How is the Big Bang Theory “proved”? It is worthwhile to contemplate this question for a minute. According to the textbooks the Big Bang Theory rests on three pillars: (1) The Hubble law relating galaxy distances to their recession velocities, which proves that our universe is expanding; (2) the cosmic microwave background (CMB) with its uniform temperature of 2.7 K; and (3) the successful prediction of the primordial abundances of small atomic nuclei during nucleosynthesis. The present **expansion rate** of our universe reflects

its **initial conditions** and the **equation of state** of the matter in the universe, integrated over its lifetime. *Primordial nucleosynthesis* happened when the universe had cooled down to about $T \simeq 100$ keV, about 3 minutes after the Big Bang; this is the stage of **chemical freeze-out** of our universe at which its original chemical composition was fixed (later to be modified inside stars by non-cosmological mechanisms). The *microwave background radiation* signals the recombination of atoms and the depletion of free charges in the early universe, rendering it transparent to photons. This **thermal freeze-out** of our universe happened much later, about 400000 years after the Big Bang when it had cooled down to $T \simeq 1$ eV $\simeq 3000$ K.

Before thermal freeze-out, the universe was in nearly perfect local and global *thermal* equilibrium (except for the neutrinos which froze out earlier and today have a temperature of 1.95 K). Before the onset of nucleosynthesis, it was also in a state of *chemical* equilibrium. Thermodynamic equilibrium being a state of maximum entropy or minimal information, all memory about the earlier stages of the universe got wiped out, leaving practically no directly observable traces. In particular, the color-confining phase transition with its formation of hadrons from quarks and gluons at about $10 \mu\text{s}$ after the Big Bang, which we now want to study in the laboratory, is in cosmology safely hidden behind the curtain of thermal CMB photons. No **direct probes** from the early stages are known which survived this tendency for re-equilibration; given the roughly 18 orders of magnitude between the (slow) expansion rate of the universe and the (fast) strong, weak and electromagnetic interaction rates among the particles this is, of course, not surprising. At the moment our best bet for direct signals from the very early universe seems to be a detailed and quantitative analysis of the **fluctuations** in the CMB spectrum which occur at the level of about 10^{-5} of the average signal.

Still, with only a single observed event and little or no direct experimental evidence about its very early stage to show, the Big Bang Theory has become the almost unanimously accepted model for the evolution of our cosmos. How can this be explained? The most important reason is, I think, the fact that we can analyze our present state (the **final state** of the “Big Bang experiment”) by making exceedingly accurate observations. This provides stringent constraints for the extrapolation backwards in time. Furthermore, general relativity, which has been tested elsewhere, provides a robust and highly reliable theory for the dynamical evolution of the cosmos, given the equation of state of the matter. And the latter again is known experimentally and theoretically to be simple during most parts of the dynamical evolution, with the exception of a few critical stages (typically near phase transitions) which correspondingly draw most of the present theoretical attention.

1.2 What is a quark-gluon plasma?

The initiated reader will not have missed the strong parallelism between the above discussion of the Big Bang and the field of relativistic heavy-ion collisions. Very similar concepts (indicated above by emphasized key-words) play a crucial role on both contexts. Why, then, do we not have a generally accepted theory for the “Little Bang”?

The main reason is the small geometric size of the object under study. Contrary to the Early Universe, the region of high density is limited to a region of at most a few 10 fm in diameter, surrounded by vacuum. Once the energy in the reaction zone begins to thermalize, it builds up pressure which leads to explosive expansion of the fireball. The associated expansion time scale is no longer 18 orders of magnitude, but only perhaps a factor 10 to 100 larger than that of the microscopic equilibration processes. This introduces basic uncertainties into dynamical evolution models which to eliminate requires hard work and many detailed tests. It is fair to say that the goal of a generally accepted “standard model of nuclear fireball dynamics” has not yet been reached.

Things would be much simpler if, as in cosmology, we were sure that hydrodynamics can be used. In fact, the conditions for creating a quark-gluon plasma (QGP) and for being able to describe its dynamics hydrodynamically are very closely related. Both involve an assessment of the degree of local equilibrium that can be reached. I would list the following criteria for being permitted to call a small, short-lived, rapidly expanding system of quarks and gluons a quark-gluon **plasma**:

1. Sufficient *energy density* for deconfinement, $\epsilon \gg \epsilon_{\text{cr}} \simeq 1 \text{ GeV/fm}^3$.
2. Locally *thermal momentum distributions* with the same temperature T for all particle species, in a limited momentum range $0 < p \lesssim 6T$. To establish collective plasma properties and to validate a hydrodynamic approach, it is not necessary to fully equilibrate the tails of the momentum distributions. In fact, given the short lifetime and small size of the reaction zone, some fast particles produced by hard QCD processes will always escape, giving a power-law tail to the momentum spectrum. Note that *chemical equilibrium* is also not necessary: the relative abundances of gluons and light and heavy (anti)quarks need not be equilibrated for plasma properties and hydrodynamic behavior to manifest themselves. Chemical non-equilibrium requires, however, the introduction of additional chemical potentials in the equation of state.
3. Sufficiently *large volume* and *strong rescattering*. This and the following

criterion are the most subtle ones: the relevant volume is characterized by the mean free path which again reflects the scattering rate. To ensure thermalization by kinetic equilibration we must require

$$\frac{V_{\text{hom}}}{\lambda_{\text{mfp}}^3} \gg 1 \quad (1)$$

where in perturbation theory the mean free path is given^{2,3} in terms of the time-dependent temperature $T(\tau) \sim \epsilon(\tau)^{1/4}$ by^a

$$\lambda_{\text{mfp}}(\tau) = \tau_{\text{scatt}}(\tau) \langle v \rangle \sim \frac{1}{\# T(\tau) \alpha^2(\tau) \ln(1/\alpha(\tau))} \quad (2)$$

(with $\#$ indicating a number proportional to the number of degrees of freedom in the plasma), and $V_{\text{hom}}(p)$ is the “homogeneity volume” of particles with momentum p :⁴

$$V_{\text{hom}}(m_{\perp}, y, \tau) = 2\pi R_{\parallel}(m_{\perp}, y, \tau) R_{\perp}^2(m_{\perp}, y, \tau). \quad (3)$$

R_{\parallel}, R_{\perp} are the longitudinal and transverse “homogeneity lengths” as measured by Bose-Einstein correlations. For thermalized expanding fireballs they can be estimated by simple analytical expressions⁴ which, assuming boost-invariant longitudinal expansion,⁵ lead to

$$\begin{aligned} V_{\text{hom}}(m_{\perp}, y, \tau) &= \frac{V_{\text{geom}}(\tau)}{\left(1 + \eta_f^2(\tau) \frac{m_{\perp}^2}{T^2}\right) \sqrt{1 + (\Delta\eta)^2(\tau) \frac{m_{\perp}^2}{T^2}}} \\ &\longrightarrow \propto V_{\text{geom}}(\tau) \left(\frac{T(\tau)}{m_{\perp}}\right)^{3/2}. \end{aligned} \quad (4)$$

Here the limit is for large m_{\perp} , $\eta_f(\tau)$ is the average transverse flow rapidity of the fireball, $\Delta\eta(\tau)$ its longitudinal extension in space-time rapidity, and $V_{\text{geom}}(\tau) = \pi R^2(\tau) \cdot 2\tau \Delta\eta(\tau)$ is the geometric fireball size (growing with time). The interesting ratio (1) then becomes

$$\frac{V_{\text{hom}}(m_{\perp}, \tau)}{\lambda_{\text{mfp}}^3(\tau)} \approx V_{\text{geom}}(\tau) T^3(\tau) \cdot \#^3 \alpha^6(\tau) \ln^3(1/\alpha(\tau)) \left(\frac{T(\tau)}{m_{\perp}}\right)^{3/2}. \quad (5)$$

Entropy conservation requires the first factor to be time-independent whereas the second factor grows with time. One sees that the criterion (1) is the more easy to fulfill the higher the initial temperature

^aThis implies a transport cross section $\sigma_{\text{trans}} \sim \alpha^2 \ln(1/\alpha)/T^2$ which grows as T decreases.

($T_0 = T(\tau_0)$), the larger the number of massless degrees of freedom in the plasma ($\#$), the more strongly they interact (α), and the smaller their transverse mass (m_\perp). Particles with large m_\perp will always be difficult to thermalize.

4. Sufficiently *long lifetime*:

$$\tau_{\text{scatt}} \simeq \frac{\lambda_{\text{mfp}}}{c} \ll \theta^{-1} = \frac{1}{\partial \cdot u} = \tau_{\text{exp}}. \quad (6)$$

The divergence of the flow velocity field $\theta(x) = \partial \cdot u(x)$ gives the local expansion rate in the fireball; it is the analog of the Hubble constant in cosmology. For d -dimensional scaling expansion it is given by $\theta^{-1} = \tau_{\text{exp}} = \tau/d$ whereas the temperature drops like $T(\tau) = T_0(\tau_0/\tau)^{d/3}$, with $T_0\tau_0 \approx 1.2$.⁵ Putting this together we find

$$\frac{\tau_{\text{scatt}}}{\tau_{\text{exp}}} = \frac{d (T_0\tau)^{d/3-1}}{\# \alpha^2(\tau) \ln(1/\alpha(\tau))}. \quad (7)$$

For $d=1$ the expansion looses and the conditions for thermalization get better and better with time; the case $d=3$ is marginal², and only the increasing coupling strength $\alpha(\tau)$ at lower temperatures works in favor of increased thermalization.⁶ Of course, after hadronization the cross sections become τ -independent while the particle density continues to decrease such that eventually thermalization stops and the particle momenta freeze out.

5. Sufficient *collectivity*, *i.e.* the number of particles inside a Debye volume should be large:

$$\rho(\tau) \mu_D^3(\tau) \gg 1. \quad (8)$$

Since perturbatively the left hand side is given essentially by $\# \alpha^{3/2}$, this criterium, like the two previous ones, requires sufficiently strong coupling α . Small values of α are certainly disadvantageous for thermalization in heavy-ion collisions; fortunately, in real life α seems to be sufficiently large (much to the dismay of the practitioners of perturbative QCD).

2 Heavy-Ion Observables: Hard and Soft Probes

The observables in relativistic heavy-ion collisions can be divided into two classes: hard and soft probes. *Hard* probes are created early in the collision and, due to the *finite size* of the reaction fireball and their relatively small reinteraction cross section, they decouple early. They include hard direct photons

and lepton pairs, hadronic jets, and charmonia ($J/\psi, \psi', \dots$). *Soft* probes are the light quark flavors u, d, s and the corresponding hadrons, as well as the soft electromagnetic radiation emitted by them. They are created throughout the collision history, and the strongly interacting ones decouple late, triggered by the *expansion* of the fireball rather than by its finite size. Soft probes include the hadron abundance ratios, their momentum spectra and their momentum correlations.

The soft probes contain equivalent information as the known signatures of the cosmological Big Bang: Hadron abundancies give information about the *chemical equilibration* time scales; here strangeness plays a crucial role since the time scale $\tau_{\bar{s}s}$ for creating strange quark pairs is roughly of the same order of magnitude as the fireball lifetime such that moderate changes in $\tau_{\bar{s}s}$ due to new physics (e.g. color deconfinement and the onset of gluon fusion⁷) can cause major effects. The hadronic momentum spectra and two-particle correlations provide information on *thermalization and collective flow*. Since flow is generated by pressure, the observed flow pattern in the final state gives a time integral of the pressure history in the fireball (and thus its equation of state), with different types of flow (radial expansion in central collisions, directed and elliptic flow in semiperipheral ones) receiving different weights from early and late dynamical stages.⁸ The observed flow patterns are thus the “Little Bang” analogues of the Hubble expansion in cosmology.

The Little Bang can therefore be reconstructed from the soft probes in very much the same way as the cosmological Big Bang; hard probes, which escape directly from the early stages of the Little Bang and for which no cosmological analogue exists (due to the absence of spatial boundaries of the universe), can then be used to check the consistency of the reconstruction. The presently available data allow for the realization of the first part of this program; the second part will require the higher collision energies becoming available at RHIC and LHC in the next few years.

3 Hard Probes: The Present Status

An extensive review of the present status of QGP signatures has just appeared.⁹ It contains a comprehensive list of original references to which I refer the reader for details.

Direct photons of other than hadronic decay origin have been searched for by the WA80, WA98 and CERES/NA45 collaborations at the CERN SPS in S+Au and Pb+Pb collisions. So far only an upper limit of about 5-7% above hadronic decay background could be established in S+Au collisions; the analysis of Pb+Pb data is still in progress. This eliminates hydrodynamic expansion

models with equations of state which do not include a phase transition to QGP or at least a strong softening of the equation of state by resonance and string excitations at high temperatures. A positive signal of thermal QGP radiation (whose rate grows with T^4) is, however, only expected at higher beam energies where larger initial temperatures can be reached. Whether it can be extracted from the hadronic background depends on the unknown transverse momentum distribution of the latter¹⁰ (which is affected by collective expansion).

An excess of dimuons in the mass region below the J/ψ has been reported, in one form or another, by the HELIOS3, NA38 and NA50 collaborations in S- and Pb-induced heavy-ion collisions. This excess appears to have a non-linear dependence on the charged hadron multiplicity (collision centrality). Its origin is presently unclear.¹¹

The CERES/NA45 collaboration has seen in S+Au and Pb+Au collisions a strong excess of e^+e^- pairs with masses $200 \text{ MeV} < m_{ee} < m_\rho$, with a non-linear multiplicity dependence and concentrated at low transverse momentum.¹² It can probably be explained by hadronic mechanisms, but requires a very

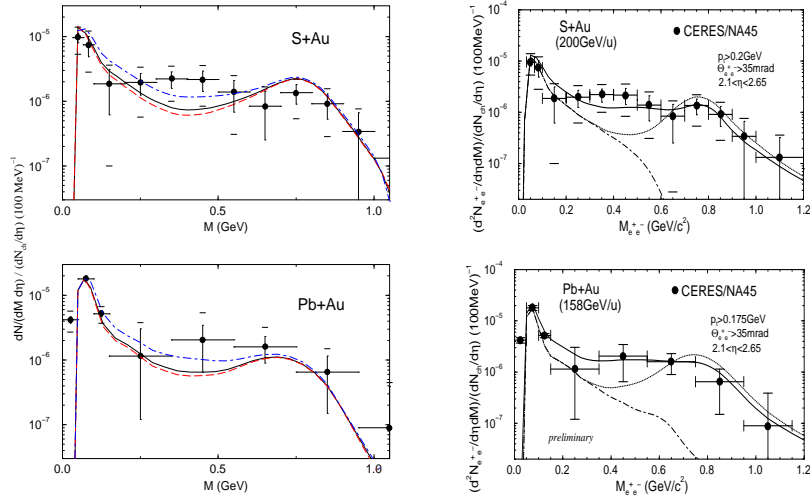


Figure 1: CERES dilepton mass spectra¹² and theoretical simulations with an expanding fireball model, using different theoretical approaches¹³ to the in-medium dilepton rates.

dense and hot hadronic medium in which pions and ρ -mesons violently rescatter, leading to a broadening of the vector meson spectral densities¹³ (Fig. 1).

Jet production and jet quenching by the dense fireball medium¹⁴ cannot be studied at present SPS energies due to insufficient rates, but will become

accessible at RHIC.

Much recent attention focussed on the discovery by NA38/NA50 of “anomalous” suppression of J/ψ and ψ' vector mesons in central nucleus-nucleus collisions. Different collision systems can be compared by introducing a theo-

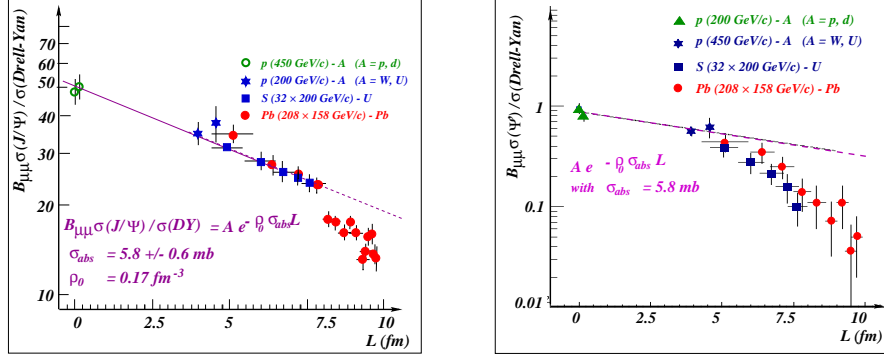


Figure 2: Preliminary data on $(J/\psi)/DY$ and ψ'/DY from the NA38/NA50 collaboration¹⁵, plotted as a function of the Glauber model nuclear thickness parameter L (see text).

retical auxiliary variable, the average path length L which the $\bar{c}c$ -pair must traverse before escaping the reaction zone.¹⁵ “Normal” suppression is defined by an exponential attenuation $B\sigma_\psi/\sigma_{DY} \propto \exp(-\rho\sigma_{abs}L)$ (straight line in Fig. 2) with the normal nuclear density ρ and a fitted ψN absorption cross section σ_{abs} . A deviation from this behaviour is first observed for the ψ' near $L = 5$ fm, then for the J/ψ near $L = 7.5$ fm. Since about 32-40% (5-8%) of the observed J/ψ stem from radiative χ_c (ψ') decays, it is not unlikely that the drop near $L = 7.5$ fm indicates anomalous χ_c suppression, and that anomalous suppression of the J/ψ itself requires even larger values of L . It is interesting that this suppression pattern follows the binding energies of the corresponding charmonium states: suppression of the more strongly bound states requires a higher density and/or lifetime of the fireball, here parametrized (perhaps not very fortunately) via L . At present the suppression mechanism is not fully understood theoretically,¹⁶ but one condition appears to be unavoidable: strong rescattering of the $\bar{c}c$ -pair in a *very dense environment*, probably of partonic origin. A consistent quantum mechanical and dynamical theory of this phenomenon is urgently needed.

4 Soft Probes: Hadronization, Thermalization and Flow

Soft hadrons, which constitute the bulk of the produced particles, provide a much richer body of experimental information which by now has been ana-

lyzed in considerable quantitative detail. As I will show, they give convincing evidence that we have seen “the Little Bang”.

4.1 Primordial hadrosynthesis

It has been known for many years that hadron production in high energy physics exhibits striking statistical features. Recently several rather detailed analyses were performed of the relative yields of different hadronic species produced in e^+e^- , pp , $p\bar{p}$ and AA collisions, with the question in mind to what extent the hadronic final state reflects a state of *chemical equilibrium*.¹⁷ The result is shown in Fig. 3.

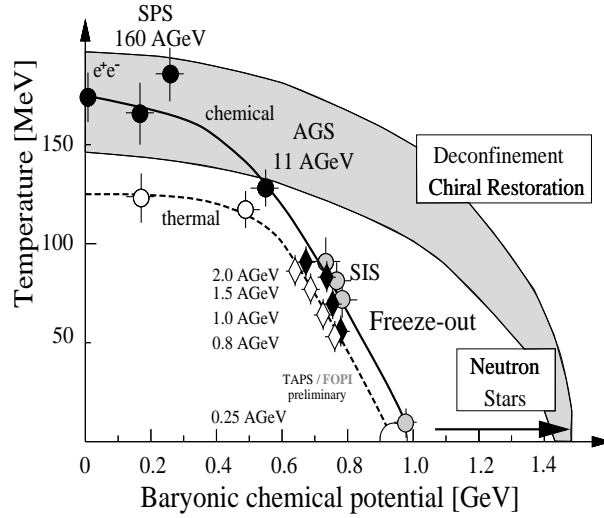


Figure 3: Compilation of freeze-out points in e^+e^- collisions and in heavy-ion collisions from SIS to SPS energies. Filled symbols: chemical freeze-out points from hadron abundances. Open symbols: thermal freeze-out points from momentum spectra and two-particle correlations. The shaded region indicates the parameter range of the expected transition to a QGP.

The single e^+e^- point represents a large number of e^+e^- , pp and $p\bar{p}$ collision systems at different center of mass energies $20 \text{ GeV} \leq \sqrt{s} \leq 900 \text{ GeV}$ which were all found¹⁸ to reflect chemical equilibrium hadron abundancies at a universal hadronization temperature $T_{\text{had}} \approx 175 \text{ MeV}$. The only clear deviation from chemical equilibrium in these systems is an undersaturation of overall strangeness, reflected in the ratio of produced strange to non-strange quark pairs $\lambda_s = 2\langle\bar{s}s\rangle/(\langle\bar{u}u\rangle + \langle\bar{d}d\rangle)|_{\text{produced}} \approx 0.2-0.25$, again almost independent

of \sqrt{s} .^{18,19} But even if the total number of $\bar{s}s$ valence quark pairs is below the chemical equilibrium value, the available s and \bar{s} quarks are distributed among the various strange hadron species according to the law of maximum entropy.

Given the small size of these collision systems it is impossible to imagine that this can be the result of equilibration by hadronic rescattering. It must reflect *pre-established* statistical equilibrium, i.e. the statistical filling of the available hadronic phase-space according to the law of Maximum Entropy at the point of hadron formation. The temperature T_{had} should be understood as a Lagrange multiplier for the energy density at which this happens; its universality and numerical value tell us that hadronization always happens at the same critical energy density $\epsilon_{\text{cr}} \approx 1 \text{ GeV/fm}^3$. At higher collision energies hadrons are not produced at higher temperatures, but over a *larger volume* at the *same energy density*.¹⁸ After formation the hadrons do *not* rescatter, and the observed hadron abundances thus reflect the *primordial* values established at the point of hadronization.

It is interesting that in heavy-ion collisions at the SPS (S+S, S+Ag, Pb+Pb) one finds again chemical equilibrium hadron abundances at the same chemical freeze-out temperature of about 180 MeV.¹⁹ This suggests hadron formation by the same statistical phase-space filling mechanism as in e^+e^- and

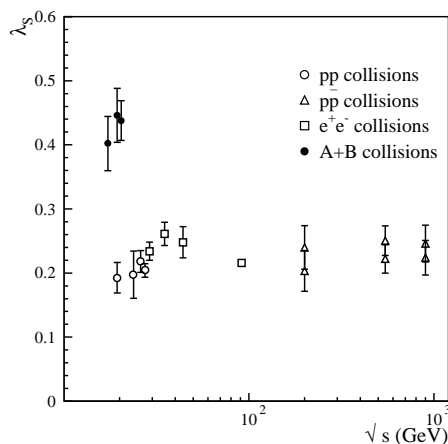


Figure 4: The strangeness suppression factor λ_s as a function of \sqrt{s} .¹⁹ The two points each for $p\bar{p}$ collisions reflect the inclusion (exclusion) of the initial valence quarks.

pp collisions (reflecting the Maximum Entropy Principle), followed by immediate freeze-out of the hadron yields. Since changes in the relative abundances require inelastic collisions whose cross sections are mostly quite small, this is not unexpected, especially if the fireball features collective expansion (which

is known to foster freeze-out) already at hadronization.

What is different from elementary collisions is that in heavy-ion collisions a considerably larger global strangeness fraction $\lambda_s \approx 0.4 - 0.45$ is measured (Fig. 4).¹⁹ Following the above argument and realizing that hadronic *strangeness-creating* cross sections are particularly small,²⁰ this can only be due to processes *before* hadronization. Indeed, all known microscopic kinetic models based entirely on pp input and hadronic reinteraction dynamics fail to reproduce this *strangeness enhancement*.²¹ Heavy-ion reactions thus generate a *prehadronic state* with different dynamics (presumably a longer lifetime) than in e^+e^- and pp collisions. The factor 2 increase in the strangeness fraction λ_s indicates a short strangeness saturation time scale $\tau_{s\bar{s}}$ in this state, as predicted for a QGP.⁷ In fact, Sollfrank²² has argued that the observed strangeness enhancement in $A + A$ collisions at the SPS is consistent with the hadronization of a *fully equilibrated* QGP at the hadronization temperature T_{had} if the hadronization process itself leaves the strangeness/entropy ratio unchanged.

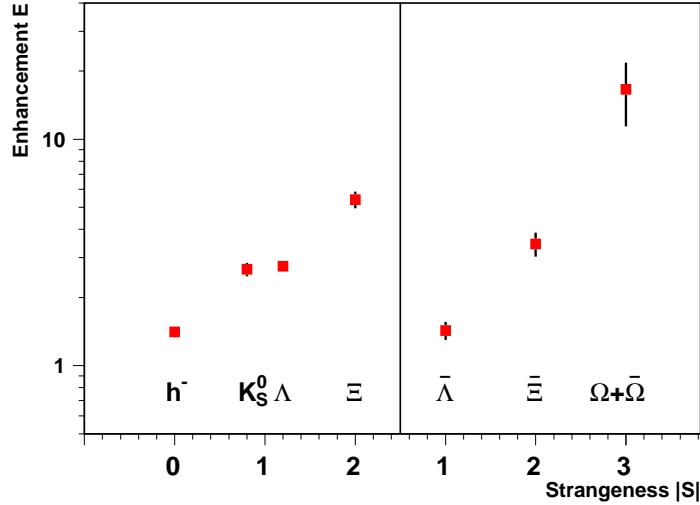


Figure 5: Enhancement factor for the mid-rapidity yields per participating nucleon in Pb+Pb relative to p+Pb collisions for various strange and non-strange hadron species.²³

The global strangeness enhancement reflected in λ_s occurs already in S+S collisions and remains roughly unchanged in Pb+Pb collisions.¹⁹ A recent comparison of p+Pb and Pb+Pb collisions at the SPS²³ (see Fig. 5) further shows that while the bulk of the strangeness enhancement is carried by the kaons and hyperons (Λ , Σ), which are enhanced by about a factor 3 near midrapidity, the

enhancement is much stronger for the doubly and triply strange baryons Ξ and Ω and their antiparticles, with an enhancement factor of about 17 (!) for $\Omega + \bar{\Omega}$ at midrapidity. Such a rise of the enhancement with the strangeness content of the hadrons is natural in statistical hadronization models, but contradicts expectations based on the respective production thresholds in hadronic (re)interactions. WA97 also found²³ that all of the enhancement factors in Pb+Pb are independent of the collision centrality, i.e. of the size of the midrapidity source, from about 100 to 400 participating nucleons, and that similar enhancement patterns are seen in S+S collisions.²³ Thus, whatever causes the enhancement in central Pb+Pb collisions exists already in S+S collisions!

The existence of a prehadronic stage without color confinement, both in S+S and Pb+Pb collisions at the SPS, is supported by a recent argument by Bialas²⁴ which generalizes similar ideas by Rafelski²⁵ by removing the assumption of thermal equilibrium. Bialas points out that by considering baryon/antibaryon production ratios the unknown baryon wave function drops out, and one can very easily test whether or not the baryons were formed by statistical hadronization (coalescence) of *uncorrelated* quarks. He finds that the data from S+S and Pb+Pb, but not those from p+Pb follow the corresponding simple “quark counting rules”; the conspicuous absence of correlations among the quarks is interpreted in terms of a color-deconfined initial state in the nuclear collisions.²⁴

While at the SPS chemical freeze-out appears to happen immediately at hadronization (such that the measured hadron yields reflect the abundances from the *primordial hadrosynthesis*), Fig. 3 suggests that at the AGS and SIS chemical freeze-out occurs at lower temperatures, after some further “chemical cooking”. This is probably due to longer lifetimes and slower expansion of the reaction zone at lower beam energies.

4.2 Thermal hadron radiation and radial flow

I now discuss the analogues of Hubble expansion and the cosmic microwave background. In heavy-ion collisions the latter is not generated by *photons* (because these decouple immediately after their production, i.e. throughout the time evolution of the fireball), but by *hadrons*. Due to their strong interactions, the fireball is *opaque* to quarks and hadrons for most of its dynamical history, and only at the end, after expansion has diluted the matter sufficiently, the hadrons decouple. As in cosmology, where, after 400000 years of complete opaqueness, the universe became transparent to photons quite suddenly after electron-ion recombination, this kinetic decoupling process appears to happen in bulk and rather suddenly also in heavy-ion collisions: two-particle Bose-

Einstein correlation measurements, which give access to the space-time structure of the fireball at the point of freeze-out,⁴ indicate for Pb+Pb collisions at the SPS an emission duration for pions (the most abundantly produced particles) of not more than 2-3 fm/c, after a total expansion time of at least 9-10 fm/c.^{26,27} Consistently with that, most of the pions are emitted from the bulk of the source and not only from a thin surface layer.^{28,29} It is also known³⁰ that in heavy-ion collisions kinetic freeze-out of hadrons is triggered by expansion, not by the finite size of the source, again as in the early universe.

What is, then, the temperature of this thermal hadron radiation? As for the cosmic microwave background, it is determined from the energy spectrum of the radiated particles and, as in the cosmological context, this energy spectrum is affected by (Hubble) expansion. Moreover, as in cosmology, the kinetic decoupling temperature reflected in the energy or momentum spectra differs from the chemical freeze-out temperature reflected in the particle abundances; it is considerably lower.

Expansion flow affects the observed momentum spectra in two distinct ways: since the source flows towards the detector, the single-particle distributions are flattened by a blueshift effect,³¹ and as different parts of the expanding source recede from each other, the homogeneity regions (Hanbury Brown/Twiss (HBT) size parameters) measured by Bose-Einstein interferometry (see Sect. 1.2) are reduced by velocity gradients in the source.^{4,27}

For the blueshift effect on single-particle transverse mass spectra one must distinguish two domains: In the region of relativistic momenta, $p_{\perp} \gg m_0$, the inverse slope T_{app} of all particle species is the same and given by the blueshift formula $T_{\text{app}} = T_f \sqrt{\frac{1+\langle v_{\perp} \rangle}{1-\langle v_{\perp} \rangle}}$. This formula does not allow to disentangle the average radial flow velocity $\langle v_{\perp} \rangle$ and freeze-out temperature T_f . In the non-relativistic domain $p_{\perp} \ll m_0$ the inverse slope is given approximately by $T_{\text{app}} = T_f + m_0 \langle v_{\perp}^2 \rangle$, and the rest mass dependence of the “apparent temperature” (inverse slope) allows to determine T_f and $\langle v_{\perp}^2 \rangle$ separately.^{31,32} (In pp collisions no m_0 -dependence of T_{app} is seen.³²)

The left diagram in Fig. 6 shows a compilation of measured slope parameters T_{app} for a variety of hadron species in Pb+Pb collisions at the SPS. While a rise with the rest mass m_0 is clearly seen, providing strong evidence for radial flow, some of the detailed features lead to ambiguities in the separation of temperature and flow. The pion slopes are very sensitive to the p_{\perp} -region in which the fits are performed, due to strong resonance decay contributions at low p_{\perp} . Also, pions are always relativistic such that the formula $T_{\text{app}} = T_f + m_0 \langle v_{\perp}^2 \rangle$ cannot be used for them,³³ and so they don’t fit very well into the systematics of that Figure. Finally, the Ω baryons (and perhaps also the Ξ ’s) exhibit steeper

slopes than expected from this formula. It was argued³⁴ that this reflects their earlier kinetic freeze-out due to an absence of strong scattering resonances with the dominating pions; these are essential for the kinetic re-equilibration of the other hadron species.

A less ambiguous separation of temperature and flow is possible by combining single-particle m_{\perp} -slopes with the pair-momentum dependence of the transverse HBT radius extracted from 2-pion correlations (right diagram in Fig. 6). The latter is approximately given by⁴ $R_{\perp}(m_{\perp}) \approx R / \sqrt{1 + \xi \langle v_{\perp}^2 \rangle \frac{m_{\perp}}{T_f}}$

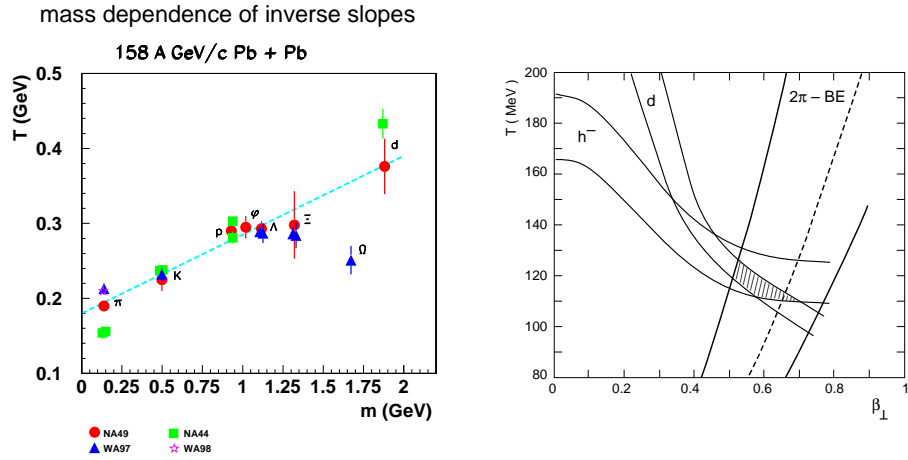


Figure 6: Left: Inverse transverse slope parameter “ T ” for different hadron species as a function of their rest masses, measured for Pb+Pb collisions at the SPS by various experiments. Right: Constraints on possible combinations of kinetic freeze-out temperature T and collective radial flow velocity β_{\perp} from the transverse momentum spectra of negative hadrons (h^{-}) and deuterons (d) and from the transverse momentum dependence of the transverse HBT radius parameter $R_{\perp}(m_{\perp})$ (2π -BE).²⁶

(see Eq. (4)) where m_{\perp} is the average transverse mass of the pions in the pair, T_f is the kinetic freeze-out temperature, and ξ is a number of order 1 which depends on the detailed transverse velocity and density profiles. Since this formula and the one for the inverse single-particle slopes provide orthogonal correlations between T_f and $\langle v_{\perp} \rangle$ (see Fig. 6), their combination leads to a rather accurate separation of both. After proper translation of the symbols one finds²⁹ for the average radial flow velocity $\langle v_{\perp} \rangle \approx 0.5c$ and for the temperature of the thermal hadron radiation $T_f \approx 100$ MeV. (The somewhat lower T_f -value than in Fig. 6 results from a more accurate fit to the single-particle h^{-} spectrum.²⁹)

Similar analyses were performed for smaller collision systems and at lower

beam energies; the results are shown by the open symbols in Fig. 3. As in the Early Universe freeze-out of the momentum spectra is seen to happen later than the decoupling of particle abundances, at significantly lower temperatures. The ability of the system to remain in a state of approximately local thermal equilibrium while building up collective expansion flow and cooling was recently demonstrated in microscopic simulations with the URQMD model.³⁵

4.3 Initial energy density

Two-particle Bose-Einstein correlation measurements give access to both the geometry and collective dynamics of the fireball at the point of kinetic freeze-out.^{4,27} One not only finds signs of strong radial flow of about $0.5c$, as just discussed, but also evidence for strong transverse *growth* of the fireball between impact and freeze-out, by more than a factor 2.³⁶ The two observations are dynamically consistent, given the lower limit on the total expansion time $\tau_f \gtrsim 8$ fm/c which can be obtained^{27,29} from the longitudinal HBT radius $R_{||}$. Knowing the freeze-out temperature T_f and collective flow velocity, the thermal and collective flow energy density of the system at freeze-out can be calculated. From the measured transverse growth factor and the known longitudinal expansion pattern (all extracted from single-particle spectra and HBT measurements) one can estimate the total geometric expansion factor of the fireball between the onset of transverse expansion and freeze-out.³⁶ Energy conservation then gives an estimate of the energy density at the beginning of transverse expansion, by multiplying the freeze-out energy density with the volume expansion factor.

This estimate has the advantage over the one using Bjorken's formula⁵ that both factors are determined more or less directly from (single-particle and correlation) measurements, thus avoiding uncontrolled model assumptions (like the identification of momentum-space with coordinate-space rapidity densities) and free parameters (as the equilibration time τ_0 in Bjorken's formula). For Pb+Pb collisions at the SPS one finds³⁶ in this way initial energy densities of $2.5 - 4$ GeV/fm³. This is comfortably above the critical energy density for deconfinement, consistent with the other arguments for an early pre-hadronic stage given above. Also, this energy density must have been at least partially thermalized because pressure (a consequence of thermalization) is necessary to drive the transverse expansion.

4.4 Elliptic flow: evidence for "early pressure"

In addition to radial transverse flow, which is typical for central collisions, two other types of collective flow occur in collisions with finite impact para-

meter: in-plane directed flow (“bounce-off”) and elliptic flow.^{37,38} While the first of these is concentrated at forward and backward rapidities, elliptic flow is strongest at midrapidity. At very high energies the directed flow becomes weak,³⁹ and only elliptic flow survives. Both types of directed flow can be identified by a harmonic analysis of the azimuthal dependence of the single-particle distributions around the beam axis, with in-plane (elliptic) directed flow given by the first (second) harmonic coefficient.³⁸

Elliptic flow arises from the initial elliptic spatial deformation of the overlap region of the two colliding nuclei in the transverse plane. If rescattering between secondaries created in this region builds up pressure sufficiently quickly, the resulting elliptic anisotropy of the pressure gradients causes an elliptic deformation in the developing flow pattern: along the shorter dimension the pressure gradient is larger and the flow develops faster. This quickly reduces the geometric deformation, i.e. the developing elliptic flow eliminates its own cause. This is the main reason why elliptic flow is particularly sensitive to the pressure and equation of state in the *early* stages of the collision whereas radial flow receives strong contributions also from the late stages.⁸

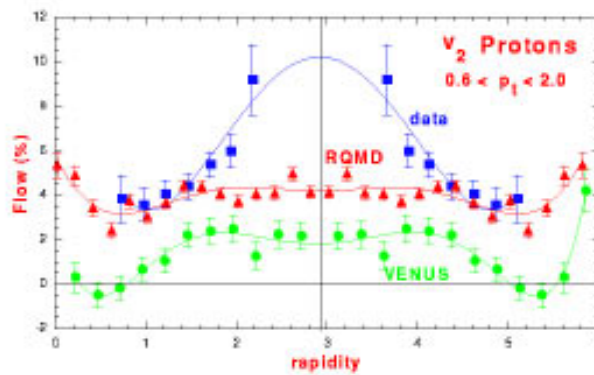


Figure 7: Second harmonic coefficient v_2 of the azimuthal distribution (elliptic flow) of protons in Pb+Pb collisions at the SPS, as a function of rapidity. NA49 data⁴⁰ are shown together with RQMD and VENUS simulations.⁴¹

Elliptic flow was measured in Pb+Pb collisions at the SPS by the NA49 collaboration.⁴⁰ Figure 7 shows the data for protons (due to their larger mass they show a stronger signal than pions⁴⁰), together with simulations using RQMD and VENUS event generators. Clearly the latter underpredict the effect significantly. This failure is due to the particular way these codes parametrize

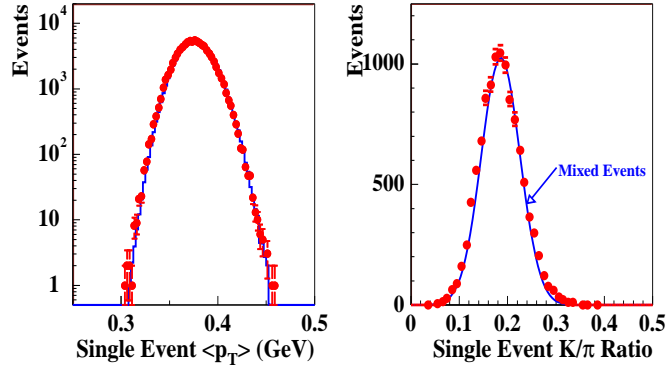
particle production: colliding nucleons create strings which, after a formation time of about 1 fm/c, decay directly into hadrons. During the initial stage of highest energy density the energy is thus stored in non-interacting strings which do not contribute to the pressure. In other words, their equation of state is “ultra-soft”.⁸

Sorge has recently shown⁸ that a modification of the RQMD code which simulates a harder QGP equation of state during the early stage is able to generate the elliptic flow signal. Moreover, he found that the *entire* effect is created during the high density stage with $\epsilon > \epsilon_{\text{cr}}$; after hadronization the elliptic flow quickly saturates.⁸ The elliptic flow data⁴⁰ can thus be viewed as a rather direct glimpse of the quark-gluon plasma.

4.5 Absence of non-statistical event-by-event fluctuations

In the introduction I mentioned that in cosmology the only direct signature from the time before chemical and thermal freeze-out seem to be the recently discovered small temperature fluctuations in the microwave background. Generated by gravitation, they have no analogue in heavy-ion physics. There,

NA49 Pb+Pb Event-by-Event Fluctuations



Dynamical Event-by-Event Fluctuations: < 1% in $\langle p_T \rangle$
< 15% in K/π

Figure 8: Event-by-event fluctuations of $\langle p_T \rangle$ and K/π in Pb+Pb collisions at the SPS.⁴³ The solid lines denote the statistical fluctuations from mixed events.

however, we can study large numbers of collision events and investigate the

fluctuations of physical observables from event to event. Such fluctuations are expected for statistical reasons because of the finite size of the collision system and the finite number of produced particles. If the collision fireballs are truly thermalized, finite number effects and quantum statistical fluctuations should be the *only* reason for event-by-event fluctuations.⁴²

Figure 8 shows the measured distributions for the average transverse momentum $\langle p_{\perp} \rangle$ and for the K/π ratio in individual Pb+Pb collision events at the SPS.⁴³ These distributions are perfect Gaussians to a level of a few times 10^{-4} ; moreover, the widths of these Gaussians agree very accurately with expectations from mixed events, i.e. the fluctuations in the measured quantities from event to event are consistent with purely statistical (e.g. thermal) fluctuations. No signs for large “critical fluctuations” expected near a phase transition or of other dynamical fluctuations are visible. If, as argued above, the chemical composition, which leads to a given average K/π ratio, and the thermalization and flow pattern, which causes a certain average transverse momentum of the emitted hadrons, reflect interesting physics of the fireball evolution, *every* Pb+Pb event at the SPS reflects it in exactly the same way, at the level of less than a permille!

5 Conclusions

I have presented arguments that in heavy-ion collisions at the SPS we have seen **THE LITTLE BANG**: the measured soft hadron spectra show convincing evidence for Hubble-like (3-dimensional) flow, for thermal (hadron) radiation, and for “primordial” hadrosynthesis out of a pre-hadronic state without quark confinement. There are strong signs for the existence of a pre-hadronic stage with non-trivial dynamics, resulting in a global strangeness enhancement by about a factor 2, in a particularly strong enhancement of multistrange (anti)baryons consistent with a statistical hadronization picture, in the suppression of J/ψ , χ_c and ψ' states, and in elliptic flow. The absence of non-statistical fluctuations from event to event indicates that all collision events are similar, that these interesting phenomena occur in every event, and that decoupling did not take place close to a phase-transition. For chemical decoupling (which I argued to happen directly after hadron formation) this implies that the hadronization process cannot be viewed as an equilibrium phase transition; thermal freeze-out was found to occur at much lower temperatures, in safe distance from any phase transition.

The abundance and quality of hadron data now available allows for a detailed and quantitative description of the final state in heavy-ion collisions. This begins to severely constrain dynamical extrapolations backward in time.

Although no *direct* signatures from the pre-hadronic stage have so far been seen, the soft hadron data leave little room for doubt that it is there. Whether we can call it a quark-gluon plasma which satisfies the criteria spelled out in Sec. 1.2 will only become clear at higher collision energies where such direct signals become accessible. At the moment we only know that the pre-hadronic state exerts pressure, so a certain degree of thermalization among the partons must have occurred. The other important open question is, of course: where is the threshold for deconfinement and how do we identify it experimentally? Clearly, much work remains to be done but now we know that we are on the right track.

Acknowledgments

I would like to warmly thank the organizers of this stimulating workshop for the invitation and for their hospitality. I am grateful to C. Slotta and B. Tomášik for help with the figures. This work was supported in part by GSI, DFG, and BMBF.

References

1. F. Karsch, *Nucl. Phys. B (Proc. Suppl.)* **60**, 169 (1998).
2. H. Heiselberg, X.-N. Wang, *Phys. Rev. C* **53**, 1892 (1996)
3. P. Arnold, L. Yaffe, this volume.
4. U.A. Wiedemann, U. Heinz, nucl-th/9901094, *Phys. Rep.*, in press.
5. J.D. Bjorken, *Phys. Rev. D* **27**, 140 (1983).
6. S.M.H. Wong, *Phys. Rev. C* **56**, 1075 (1997); *Nucl. Phys. A* **638**, 527c (1998)
7. J. Rafelski, B. Müller, *Phys. Rev. Lett.* **48**, 1066 (1982).
8. H. Sorge, *Phys. Lett. B* **402**, 251 (1997); nucl-th/9812057.
9. S.A. Bass, M. Gyulassy, H. Stöcker, W. Greiner, *J. Phys. G* **25**, R1 (1999).
10. P.V. Ruuskanen, in: *Particle Production in Highly Excited Matter*, (H.H. Gutbrod, J. Rafelski, eds.), NATO ASI Series B **303** (1993) 593 (Plenum, New York).
11. E. Scapparini et al. (NA38/NA50 Coll.), *J. Phys. G* **25**, 235 (1999).
12. I. Ravinovich et al. (CERES Coll.), *Nucl. Phys. A* **638**, 159c (1998).
13. J. Wambach, R. Rapp, *Nucl. Phys. A* **638**, 171c (1998).
14. X.-N. Wang, *Phys. Rep.* **280**, 287 (1997).
15. L. Ramello et al. (NA50 Coll.), *Nucl. Phys. A* **638**, 261c (1998).
16. D. Kharzeev, *Nucl. Phys. A* **638**, 279c (1998).
17. U. Heinz, *J. Phys. G* **25**, 263 (1999), and references therein.

18. F. Becattini, *Z. Phys. C* **69**, 485 (1996); *J. Phys. G* **25**, 287 (1999); F. Becattini and U. Heinz, *Z. Phys. C* **76**, 269 (1997).
19. F. Becattini, M. Gaździcki, J. Sollfrank, *Eur. Phys. J. C* **5**, 143 (1998).
20. P. Koch, B. Müller, J. Rafelski, *Phys. Rep.* **142**, 167 (1986).
21. G.J. Odyńec, *Nucl. Phys. A* **638**, 144c (1998).
22. J. Sollfrank, F. Becattini, K. Redlich, H. Satz, *Nucl. Phys. A* **638**, 399c (1998).
23. E. Andersen et al. (WA97 Coll.), *Phys. Lett. B* **433**, 209 (1998); *J. Phys. G* **25**, 171, 181, and 209 (1999).
24. A. Bialas, *Phys. Lett. B* **442**, 449 (1998).
25. J. Rafelski, *Phys. Lett. B* **262**, 333 (1991).
26. H. Appelshäuser et al. (NA49 Coll.), *Eur. Phys. J. C* **2**, 661 (1998).
27. U. Heinz, B.V. Jacak, *Ann. Rev. Nucl. Part. Sci.* **49** (1999), in press (nucl-th/9902020).
28. B. Tomášik, U. Heinz, nucl-th/9805016.
29. B. Tomášik, PhD thesis, University of Regensburg, Feb. 1998; and to be published.
30. E. Schnedermann, U. Heinz, *Phys. Rev. C* **50**, 1675 (1994).
31. K.S. Lee, U. Heinz, E. Schnedermann, *Z. Phys. C* **48**, 525 (1990).
32. N. Xu et al. (NA44 Coll.), *Nucl. Phys. A* **610**, 175c (1996).
33. J.R. Nix, *Phys. Rev. C* **58**, 2303 (1998).
34. H. van Hecke, H. Sorge, N. Xu, *Phys. Rev. Lett.* **81**, 5764 (1998).
35. L.V. Bravina et al., *J. Phys. G* **25**, 351 (1999).
36. U. Heinz, in *QCD Phase Transitions* (H. Feldmeier et al., eds.), Proc. 25th International Workshop on Gross Properties of Nuclear and Nuclear Excitations, Hirschegg, Jan. 13-18, 1997, GSI Report, p. 361; and in *Relativistic Aspects of Nuclear Physics* (T. Kodama et al., eds.; World Scientific, Singapore, 1998), p. 19.
37. H. Stöcker, W. Greiner, *Phys. Rep.* **137**, 277 (1986).
38. J.-Y. Ollitrault, *Phys. Rev. D* **48**, 1132 (1993).
39. D.H. Rischke et al., *Heavy Ion Phys.* **1**, 309 (1995); D.H. Rischke, M. Gyulassy, *Nucl. Phys. A* **597**, 701 (1996).
40. H. Appelshäuser et al. (NA49 Coll.), *Phys. Rev. Lett.* **80**, 4136 (1998).
41. A. Poskanzer and NA49 Collaboration, private communication, April 1998.
42. S. Mrówczyński, M. Gaździcki, *Z. Phys. C* **54**, 127 (1992); S. Mrówczyński, *Phys. Lett. B* **439**, 6 (1998).
43. G. Roland et al. (NA49 Coll.), *Nucl. Phys. A* **638**, 91c (1998).